

MIT Open Access Articles

Driven electronic states at the surface of a topological insulator

The MIT Faculty has made this article openly available. **Please share** how this access benefits you. Your story matters.

Citation: Fregoso, Benjamin M., Y. H. Wang, N. Gedik, and Victor Galitski. "Driven Electronic States at the Surface of a Topological Insulator." Phys. Rev. B 88, no. 15 (October 2013). © 2013 American Physical Society

As Published: <http://dx.doi.org/10.1103/PhysRevB.88.155129>

Publisher: American Physical Society

Persistent URL: <http://hdl.handle.net/1721.1/88758>

Version: Final published version: final published article, as it appeared in a journal, conference proceedings, or other formally published context

Terms of Use: Article is made available in accordance with the publisher's policy and may be subject to US copyright law. Please refer to the publisher's site for terms of use.



Driven electronic states at the surface of a topological insulator

Benjamin M. Fregoso,^{1,2} Y. H. Wang,^{3,4} N. Gedik,³ and Victor Galitski²

¹*Department of Physics, University of California, Berkeley, Berkeley CA 94720, USA*

²*Joint Quantum Institute and Condensed Matter Theory Center, Department of Physics, University of Maryland, College Park, Maryland 20742-4111, USA*

³*Department of Physics, Massachusetts Institute of Technology, Cambridge, Massachusetts 02139, USA*

⁴*Department of Applied Physics, Stanford University, Stanford, California 94305, USA*

(Received 29 May 2013; revised manuscript received 11 August 2013; published 23 October 2013)

Motivated by recent photoemission experiments on the surface of topological insulators we compute the spectrum of driven topological surface excitations in the presence of an external light source. We completely characterize the spectral function of these nonequilibrium electron excitations for both linear and circular polarizations of the incident light. We find that in the latter case, the circularly polarized light gaps out the surface states, whereas linear polarization gives rise to an anisotropic metal with multiple Dirac cones. We compare the sizes of the gaps with recent pump-probe photoemission measurements and find good agreement. We also identify theoretically several new features in the time-dependent spectral function, such as shadow Dirac cones.

DOI: [10.1103/PhysRevB.88.155129](https://doi.org/10.1103/PhysRevB.88.155129)

PACS number(s): 79.60.Jv, 73.21.-b, 78.67.-n, 72.20.Ht

I. INTRODUCTION

Topological properties of matter usually manifest in the appearance of electronic states at the boundary.¹ An especially interesting class of such topological boundary modes arises in three-dimensional (3D) topological insulators (TI) which have now been detected experimentally in several material systems.²⁻⁶ The edge states consist of fermions in 2D with linear dispersion relation and where its spin and momenta have a fixed relative orientation. Recently, a new possibility for creating topological band structures in nonequilibrium was suggested,⁷⁻⁹ where an initially topologically trivial semiconductor is converted into a topological insulator via an external irradiation. The resulting state was dubbed a Floquet topological insulator and an analog to such a state was recently realized experimentally in a photonic system.¹⁰ In the same vein, other theoretical works¹¹⁻¹³ have studied the realization of a lattice quantum Hall state with time-periodic perturbations.

The focus of these previous studies has been on turning an electronic system with a topologically trivial band structure into a topological insulator by subjecting it to a periodic-in-time perturbation. Here, on the contrary, we study the effect of an external irradiation on an initially topological state. The motivation comes from the development of new experimental probes that make it possible to access the time-resolved excitation spectrum of driven electrons at the surface of TIs using time-resolved photoemission spectroscopy.¹⁴ Below, we focus specifically on the properties of driven Dirac electrons on the surface of existing 3D topological materials such as $\text{Bi}_x\text{Sb}_{1-x}$ alloy, Bi_2Te_3 , and Bi_2Se_3 (Ref. 15). We are particularly interested in describing the modification of the spectrum of the boundary modes due to the irradiation as a function of the parameters of the incident light. The spectrum is composed of Floquet bands of the driven Dirac Hamiltonian, as discussed in the previous related works Refs. 12 and 16–18. Besides, proving the existence of new dynamical Dirac cones which can be engineered, we also unify and extend previous analysis and apply our results specifically to describe an experiment which observed an induced energy gap in driven surface states of Bi_2Se_3 using time- and- angle-resolved

photoemission spectroscopy (TrARPES), Ref. 19. We find that our results fit the data well.

II. MODEL OF DRIVEN SURFACE STATES

We consider noninteracting electrons at the surface of a TI with incident light normal to the surface. The Hamiltonian is

$$H(\mathbf{k}, t) = H_0(\mathbf{k}) + H_{\text{ext}}(t), \quad (1)$$

$$H_0(\mathbf{k}) = v(k_x\sigma_y - k_y\sigma_x), \quad (2)$$

$$H_{\text{ext}}(t) = V\Theta(t - t_0)[a_x(t)\sigma_y - a_y(t)\sigma_x]. \quad (3)$$

$H_{\text{ext}}(t)$ describes the external radiation source. The electrons are minimally coupled by the Peierls substitution $\mathbf{k} \rightarrow \mathbf{k} + e\mathbf{A}(t)$, where $\mathbf{A}(t) = A_0\mathbf{a}(t)$ is the vector potential. We have set $\hbar = 1$, $c = 1$, the scalar potential to zero, and ignored small magnetic effects. Two polarizations are considered $\mathbf{a}(t) = (\pm \cos \Omega t, \sin \Omega t)$ (circular) and $\mathbf{a}(t) = (\cos \Omega t, 0)$ (linear), where $T = 2\pi/\Omega$ is the period of the external perturbation. The energy scale of the perturbation is given by $V = evA_0 = evE_0/\Omega$, where E_0 is the amplitude of the electric field and v the speed of Dirac fermions. The dimensionless coupling constant V/Ω characterizes the strength of the perturbation. We assume the photon energies are small compared with the bulk gap of the TI (<300 meV).

The evolution operator, which is a 2×2 matrix, obeys the time-dependent Schrödinger equation $i\partial_t U_{\mathbf{k}}(t, t') = H(\mathbf{k}, t)U_{\mathbf{k}}(t, t')$, with initial condition $U_{\mathbf{k}}(t, t) = 1$. Once the evolution operator is known, all other correlators can be calculated in terms of the initial state of the system. We first compute the retarded Green's function in terms of the evolution operator using the equations of motion for the $c_{\mathbf{k},\alpha}$ fields yielding the expression $g_{\alpha\beta}^r(\mathbf{k}, t, t') \equiv -i\Theta(t - t')\langle\{c_{\mathbf{k}\alpha}(t), c_{\mathbf{k}\beta}^\dagger(t')\}\rangle = -i\Theta(t - t')U_{\mathbf{k}\alpha\beta}(t, t')$, where $U_{\mathbf{k}\alpha\beta}$ is the (α, β) matrix element of $U_{\mathbf{k}}$. We can similarly compute the nonequilibrium electron distribution from the two-time lesser Green's function which in terms of the evolution operator would read as $g_{\alpha\beta}^<(\mathbf{k}, t, t') \equiv i\langle c_{\mathbf{k}\beta}^\dagger(t')c_{\mathbf{k}\alpha}(t) \rangle = iU_{\mathbf{k}\gamma\beta}^\dagger(t', t_0)\langle c_{\mathbf{k}\gamma}^\dagger(t_0)c_{\mathbf{k}\delta}(t_0) \rangle U_{\mathbf{k}\alpha\delta}(t, t_0)$ (summation over repeated indices is implied and Greek indices

take values $\{1,2\}$). We now make the simplifying assumption that a quasi-steady-state has been reached, or equivalently that all correlations due to the initial state of the system had been washed away (mathematically we set $t_0 = -\infty$). Then the form of the evolution operator can be obtained analytically. Indeed, the evolution operator is T -periodic $U_{\mathbf{k}}(t+T, t'+T) = U_{\mathbf{k}}(t, t')$ and hence the retarded Green's function also becomes T -periodic in the average time variable $\bar{t} = (t+t')/2$. This periodic structure allows for a simple analytical expression of the Wigner representation²⁰ of the retarded Green's function. Here we focus on the pole structure of the nonequilibrium retarded Green's function in the Wigner representation which in a sense is similar to the Lehmann representation of equilibrium correlators.

III. SPECTRAL FUNCTION

It can be shown that the evolution operator²¹ $U_{\alpha\beta}(t, t') = \sum_{nm\gamma} \langle \alpha n | \phi_{\gamma}^m \rangle \langle \phi_{\gamma}^m | \beta 0 \rangle e^{-i\epsilon_{\gamma m}(t-t') + in\Omega t}$, satisfies the Schrödinger equation where $\langle \alpha n | \phi_{\gamma}^m \rangle$ represents the (α, n) component of the eigenvector $|\phi_{\gamma}^m\rangle$ of the Floquet Hamiltonian. Hence Fourier transforming in \bar{t} and relative time $t-t'$ the Wigner representation of the retarded Green's function is,

$$g_{\alpha\beta}^r(\mathbf{k}, n, \omega) = \sum_{\gamma m} \frac{\langle \alpha n | \phi_{\mathbf{k}\gamma}^m \rangle \langle \phi_{\mathbf{k}\gamma}^m | \beta 0 \rangle}{\omega - \epsilon_{\mathbf{k}\gamma m} + n\Omega/2 + i0^+}. \quad (4)$$

One can similarly obtain simple expressions for the inverse of the retarded Green's function by noting that $U_{\mathbf{k}}(t, t')^{-1} = U_{\mathbf{k}}(t', t)$. Driven systems on a lattice with one band have been studied before.²² The important point is that single-particle excitations, which occur at the poles of the imaginary part of the retarded Green's function, are given by the quasienergies of the driven Dirac Hamiltonian, Eq. (1). The index n in Eq. (4) represents the number of photons interacting with the Dirac electron. For example, a one-photon resonant transition creates excited states shifted by $\pm\Omega/2$ with respect to the original Dirac bands $\pm vk$ (see Appendix D). This dependence on n was not considered in Ref. 11.

We are interested in the single-particle excited states which are given by the singularities of the nonequilibrium spectral function. In the Wigner representation it is given by

$$A(\mathbf{k}, n, \omega) = -2\text{ImTr}[g^r(\mathbf{k}, n, \omega)] \\ = -2\text{Im} \left[\sum_{\gamma m} \frac{\langle \alpha 0 | \phi_{\mathbf{k}\gamma}^m \rangle \langle \phi_{\mathbf{k}\gamma}^m | \alpha 0 \rangle}{\omega - \epsilon_{\mathbf{k}\gamma m} + n\Omega/2 + i0^+} \right]. \quad (5)$$

Of particular interest is the average over a period T of the driving force which is just the $n=0$ term,

$$A(\mathbf{k}, 0, \omega) = 2\pi \sum_{\alpha\gamma m} |\langle \alpha 0 | \phi_{\mathbf{k}\gamma}^m \rangle|^2 \delta(\omega - \epsilon_{\mathbf{k}\gamma m}). \quad (6)$$

Using the completeness of the $|\phi_{\mathbf{k}\gamma}^m\rangle$ states we can verify that it satisfies the sum rule $\int (d\omega/2\pi) A(\mathbf{k}, 0, \omega) = 2$. Such property is not shared by any other moment of the nonequilibrium spectral function. In equilibrium, the spectral function does satisfy this sum rule which, in that case, derives from fermion conservation and the factor of two comes from the spin. In this sense, the average calculated above is more physical than the nonequilibrium spectral function by itself.

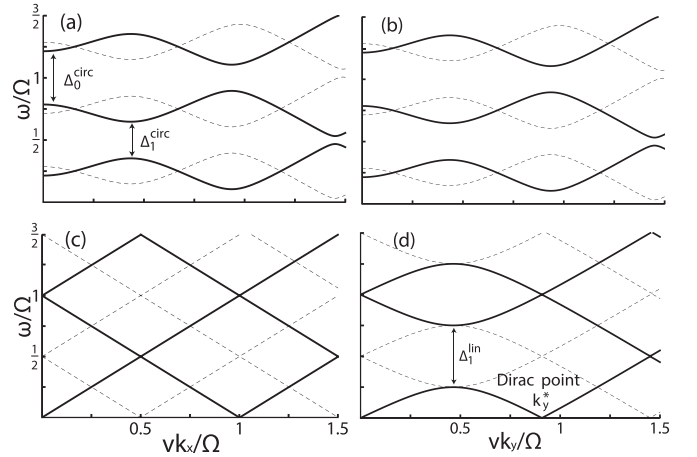


FIG. 1. Spectrum calculated using an effective Floquet Hamiltonian truncated to six modes for circular [(a), (b)] and linear [(c), (d)] polarization, with momentum along k_x [(a), (c)] and along k_y [(b), (d)]. The gap structure is clearly visible. Dashed (solid) lines are periodic (static) bands with photon index n odd (even). Here we take $V/\Omega = 0.52$, which can be achieved experimentally. Note the Bloch-Siegert shifts in (a), (b), and (d).

We now consider the general structure of $\epsilon_{\mathbf{k}\alpha n}$. See Appendix A and similar spectra obtained for irradiated graphene.^{12,16,17} One can usually find an approximate form of the quasienergies from a truncated Floquet Hamiltonian, $\langle \alpha n | \mathcal{H}_F | \beta m \rangle = H_{\alpha\beta}^{n-m} + n\Omega\delta_{\alpha\beta}\delta_{nm}$. For example, in Fig. 1 we show the quasienergies for circular and linear polarizations with six modes as a function of momentum along k_x and k_y (see also Fig. 3). We verified that higher modes do not change the spectrum significantly in the range of energies we consider. One can understand the structure of the spectrum as composed of copies of the original Dirac bands shifted by multiples of Ω , i.e., $\epsilon_{\mathbf{k}1n}^0 = vk + n\Omega$, $\epsilon_{\mathbf{k}2m}^0 = -vk + m\Omega$, and treating the effects of nonzero V perturbatively at the crossings.²¹ If there is a nonzero coupling, the bands exhibit an anticrossing (avoided crossing). For $V=0$ note that \mathcal{H}_F has time-reversal invariance and obviously time-translation invariance. We will see how these symmetries will be explicitly broken by the perturbation. In general, band crossings are associated with symmetries of the system. If there are no symmetries, any crossings/degeneracies are accidental. An early result of Von Neumann and Wigner for time-independent Hamiltonians established that two (three) parameters are necessary to produce an accidental degeneracy for real (complex) Hamiltonians. Hence by varying only one parameter, such as k_x or k_y , we expect to produce only avoided crossings.

Consider the case of circularly polarized photons. In this case time-reversal symmetry is broken, and since no other symmetries remain we expect only avoided crossings in the spectrum [Figs. 1(a) and 1(b)]. If the perturbation is small, $V/\Omega \ll 1$, we can restrict the analysis to the two crossing bands in question. For concreteness, consider the crossing at $vk_x \approx \Omega/2$ and $k_y = 0$. The effective Hamiltonian is

$$H_{2vk_x=\Omega} = \begin{pmatrix} H_0 + \Omega & iV\sigma^- \\ -iV\sigma^+ & H_0 \end{pmatrix}, \quad (7)$$

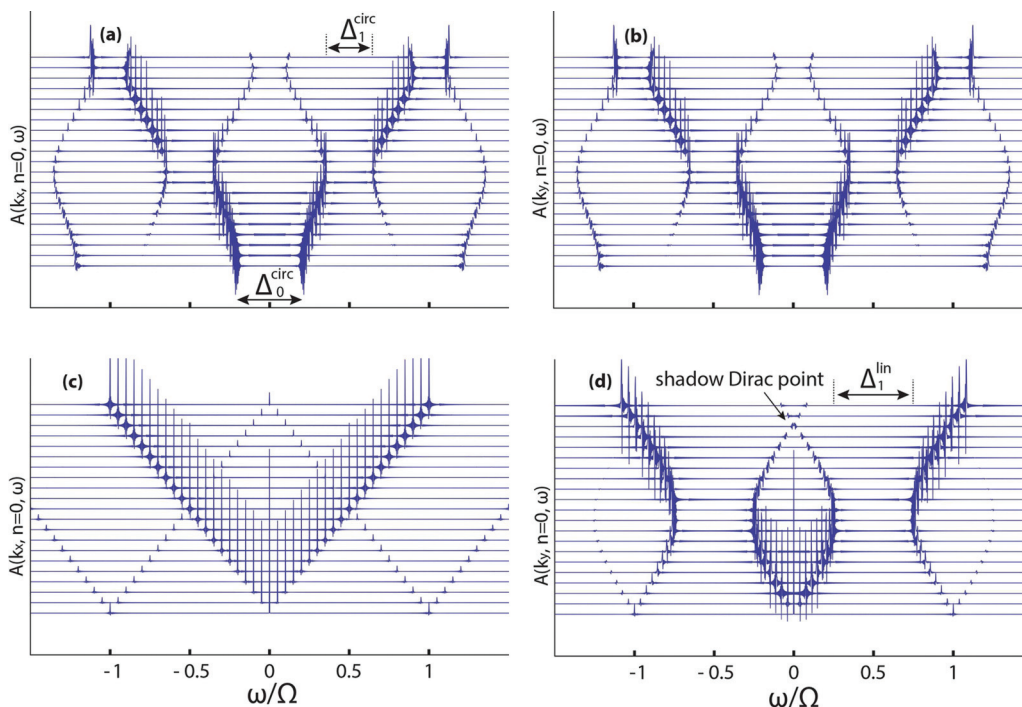


FIG. 2. (Color online) Average of the spectral function, $A(\mathbf{k}, n=0, \omega)$, from numerically evolving the evolution operator in time, Fourier transforming and taking the imaginary part of the retarded Green function. We consider circular [(a), (b)] and linear [(c), (d)] polarization, with momentum along the k_x axis [(a), (c)] and k_y axis [(b), (d)]. In all panels, the horizontal lines correspond to different values of k_x (k_y) from $k_x = 0$ ($k_y = 0$) to $vk_x = \Omega$ ($vk_y = \Omega$) in steps of 0.05. We see the photoinduced gaps at the Dirac point and finite momentum. An exact crossing occurs at k_y^* with linear polarization, panel (d), giving rise to a shadow Dirac point. For $V/\Omega = 0.52$, the spectral weight is concentrated near the original Dirac bands but significant weight is still observed at shadow bands which are displaced by multiples of Ω . From the graphs we can read $\Delta_0^{\text{circ}} = 0.43\Omega$, $\Delta_1^{\text{circ}} = 0.31\Omega$ and $\Delta_0^{\text{lin}} = 0$, $\Delta_1^{\text{lin}} = 0.52\Omega$.

where we used $H_{\text{ext}}(t) = iV\sigma^- e^{i\Omega t} + \text{h.c.}$ and $\sigma^\pm = (\sigma_x \pm i\sigma_y)/2$. In the absence of the external perturbation, the four eigenvalues of the above matrix are vk_x , $-vk_x$, $vk_x + \Omega$, and $-vk_x + \Omega$ corresponding to the eigenvalues of the diagonal terms. Note that for $V = 0$ two of these bands cross at $vk_x = \Omega/2$. The effect of a small nonzero V/Ω is to open a gap in the spectrum at $vk_x = (\Omega/2)\sqrt{(2V^2 + \Omega^2)/(V^2 + \Omega^2)}$ of magnitude $\Delta_1^{\text{circ}}/\Omega = V/\sqrt{V^2 + \Omega^2} = V/\Omega + O(V^3)$. The magnitude of this gap agrees with previous perturbative calculations using the rotating wave approximation.¹⁶ For larger V/Ω , where the above approximation of retaining just two modes is not valid, the resonance occurs at momenta $vk_x < \Omega/2$ [see Figs. 1(a) and 1(b)]. An exact numerical solution of the time-dependent Schrödinger equation confirms this result as shown in Figs. 2(a) and 2(b). The Bloch-Siegert shift²³ observed is an effect beyond the scope of the rotating wave approximation.

Next we consider the Dirac point where a gap is photoinduced¹² due to the absorption and subsequent emission of a photon by an electron near the Dirac point. The effective Hamiltonian is

$$H_{\mathbf{k}=0} = \begin{pmatrix} H_0 + \Omega & iV\sigma^- & 0 \\ -iV\sigma^+ & H_0 & iV\sigma^- \\ 0 & -iV\sigma^+ & H_0 - \Omega \end{pmatrix}. \quad (8)$$

In the limit of $V/\Omega \ll 1$ the gap is $\Delta_0^{\text{circ}} \approx 2(V^2/\Omega)$ (see Appendix C). Here we provide an alternative derivation, valid to all orders in perturbation theory, by noting that at the Dirac point, the Hamiltonian in Eq. (1) is one of the few analytically solvable driven two-level models,²⁴ formally equivalent to a spin-1/2 in a circularly polarized magnetic field. Explicitly, the evolution operator at $\mathbf{k} = 0$ is given by $U_{\mathbf{k}=0}(t, t') = e^{-i\sigma_z \Omega t/2} e^{-iH(t-t')} e^{i\sigma_z \Omega t'/2}$, where $H = V\sigma_y - \Omega\sigma_z/2$. Hence the gap at the Dirac point is¹²

$$\Delta_0^{\text{circ}} = \sqrt{\Omega^2 + 4V^2} \bmod \Omega. \quad (9)$$

IV. SHADOW DIRAC POINTS

In Figs. 1(c) and 1(d), we see band crossings at $\mathbf{k} = 0$ and at finite momentum. In this section we show that these crossings are protected by a *dynamical* symmetry of the system in the presence of light with linear polarization. The Floquet operator for polarization along x , in the basis of eigenvectors of H_0 , is

$$\tilde{H}_F^{\text{lin}} = v|\mathbf{k}|\sigma_z + V \cos \varphi_{\mathbf{k}} \cos(\Omega t)\sigma_z - V \sin \varphi_{\mathbf{k}} \cos(\Omega t)\sigma_y - i\partial_t, \quad (10)$$

where $\varphi_{\mathbf{k}}$ denotes the angle between the momenta and the x -axis. If the momentum is along k_x , the external perturbation commutes with H_0 and produces the trivial spectrum shown in Fig. 1(c) with Dirac points at $vk_x = n\Omega$. If the momentum is perpendicular to the polarization the Hamiltonian is

$\tilde{\mathcal{H}}_F^{\text{lin}} = v|k_y|\sigma_z - V \cos \Omega t \sigma_y - i \partial_t$ and satisfies

$$\hat{P} \tilde{\mathcal{H}}_F^{\text{lin}} \hat{P}^{-1} = \tilde{\mathcal{H}}_F^{\text{lin}}, \quad (11)$$

where $\hat{P} = \sigma_z e^{(T/2)\partial_t}$ is the ‘‘parity’’ operator.²⁵ This operator shifts time by $t \rightarrow t + T/2$ and flips the spin operator $\sigma_y \rightarrow -\sigma_y$. This means that eigenstates $\phi_{\alpha n}$ can be defined with good parity quantum number according to whether $\alpha + n$ is even or odd. In other words, the external perturbation does not have matrix elements between states of different symmetries and hence crossings of these bands cannot be gapped; they are symmetry protected. This can be explicitly shown by writing $\tilde{\mathcal{H}}_F^{\text{lin}}$ in frequency space, in the basis of eigenvectors of H_0 , and noting that it splits into disjoint blocks $\tilde{\mathcal{H}}_F^{\text{lin}} = \tilde{\mathcal{H}}_{\text{even}} \oplus \tilde{\mathcal{H}}_{\text{odd}}$ (see Appendix B). One implication is that the $\mathbf{k} = 0$ point remains gapless,

$$\Delta_0^{\text{lin}} = 0, \quad (12)$$

to all orders in perturbation theory, as the bands $\epsilon_{\mathbf{k}1,0}, \epsilon_{\mathbf{k}2,0}$ have different parities. Indeed, at this point the Floquet operator vanishes for linear polarization.

Similarly, there are symmetry-protected band crossings at finite momentum between the bands $\epsilon_{\mathbf{k}1,\text{odd}}$ and $\epsilon_{\mathbf{k}2,\text{odd}}$. This is made explicit in Fig. 1(d), where the bands $\epsilon_{\mathbf{k}1,-1}$ and $\epsilon_{\mathbf{k}2,1}$ cross at $\pm k_y^*$. Including $n = 0, \pm 1, \pm 2$ Fourier modes we obtain zero-energy eigenvalues of $\mathcal{H}_F^{\text{lin}}$ at momenta $vk_y^*/\Omega = [10 - 2(V/\Omega)^2 - \sqrt{(V/\Omega)^4 + 8(V/\Omega)^2 + 36}]^{1/2}/2$. This expression is accurate to $O(V^2)$, i.e.,

$$\frac{vk_y^*}{\Omega} = 1 - \frac{V^2}{3\Omega^2} + O(V^4). \quad (13)$$

For $V/\Omega = 0.52$ we have $vk_y^*/\Omega \approx 0.91$. As momentum increases, with fixed $V/\Omega < 1$, the crossings asymptotically move²⁵ towards $vk_y^* = n\Omega$. On the other hand, the crossing of the $\epsilon_{\mathbf{k}1,0}$ and $\epsilon_{\mathbf{k}2,1}$ bands can be gapped because they belong to the same symmetry class. The magnitude of this gap is $\Delta_1^{\text{lin}} = V$ for $V/\Omega \ll 1$. For arbitrary direction in momentum space, other than k_x and k_y , the states have no well-defined parity, degeneracies are not symmetry-protected, and gaps develop in the spectrum (see Fig. 3). The above considerations show that band touchings occur only at these special points in momentum space and that the existence and position of these points can be *engineered* with a properly chosen frequency.

V. DISCUSSION AND CONCLUSION

In a TrARPES experiment, the measured photocurrent is proportional to the two-time (nonequilibrium) lesser Green’s function,²⁶ which in turn is proportional to the distribution function (generally unknown) and the spectral function. Furthermore, for a system where there is no phase coherence between the pump and probe pulses, we expect the photocurrent to time-average over the period of the driving force. These arguments suggest that the measured spectrum would be characterized qualitatively by the average of the spectral function, Eq. (6) (calculated numerically in Fig. 2). For concreteness, if the electric field is $E_0 \approx 2.2 \times 10^7$ V/m and the photon energies are 120 meV then using $v = 5 \times 10^5$ m/s as the speed of Dirac electrons on the surface of Bi_2Se_3 , we

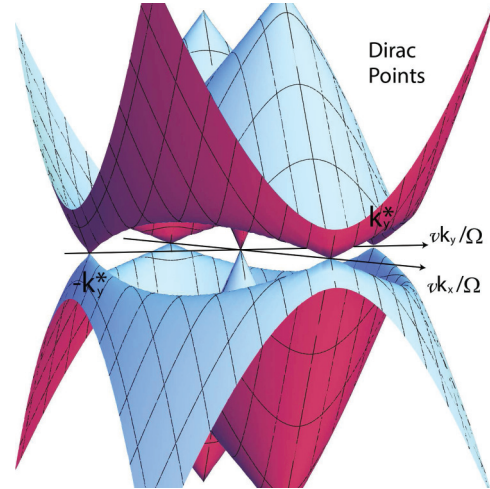


FIG. 3. (Color online) The lowest branch of the quasienergies $\pm\epsilon_{\mathbf{k}1,0}$ for linear polarization. The original Dirac cone and the anisotropic shadow Dirac cones are clearly visible. Other Dirac points can be seen in higher branches. The parameters are the same as those used in Figs. 1(c) and 1(d).

obtain a coupling $V/\Omega = 0.52$. Using Eq. (9), we obtain a gap $\Delta_0^{\text{circ}} = 51$ meV, in agreement with our simulation in Fig. 2(a) and the experiment,¹⁹ $\Delta_0^{\text{circ}} = 53 \pm 4$ meV. At finite momentum and circular polarization, we obtain $\Delta_1^{\text{circ}} = 37$ meV along k_x and k_y , and so the spectrum is isotropic [see Figs. 2(a) and 2(b)]. For linear light, we obtain $\Delta_0^{\text{lin}} = 0$ along k_x and k_y [Figs. 2(c) and 2(d)]. At finite momenta, $\Delta_1^{\text{lin}} = 0$ along k_x but $\Delta_1^{\text{lin}} = 62$ meV at $vk_y \approx \Omega/2$, in agreement with the experiment¹⁹ $\Delta_1^{\text{lin}} = 62 \pm 5$ meV. The position of the first shadow Dirac point is $vk_y^* = 109$ meV.

In conclusion, we have calculated the nonequilibrium spectral function of electrons at the surface of TIs in the presence of an incident light with circular and linear polarization. Depending on the polarization, the system is an anisotropic metal with multiple Dirac cones or an insulator. This theory along with the experimental technique would allow for optical engineering of nonequilibrium spectra in topological materials.

Note added. After completion of this work we learned about Ref. 27 which contains partial overlap with our work.

ACKNOWLEDGMENTS

We thank Jim Freericks, Kostya Kechedzhi, Stefan Natu, and Lev Bishop for discussions. Y.H.W. and N.G. would like to acknowledge support from Department of Energy Office of Basic Energy Sciences Grant No. DE-FG02-08ER46521, B.M.F. the NSF through the PFC@JQI and Conacyt, and V.G. DOE-BES (DESC0001911).

APPENDIX A: PERIODICALLY DRIVEN TWO-LEVEL HAMILTONIANS

Here we provide a brief review of periodically driven two-level systems.²¹ If the Hamiltonian is periodic in time $H(\mathbf{k}, t + T) = H(\mathbf{k}, t)$, with period T , the solution of the Schrödinger

equation

$$i \partial_t \psi_{\mathbf{k}}(t) = H(\mathbf{k}, t) \psi_{\mathbf{k}}(t) \quad (\text{A1})$$

can always be written as

$$\psi_{\mathbf{k}}(t) = \phi_{\mathbf{k}}(t) e^{-i\epsilon_{\mathbf{k}} t}, \quad (\text{A2})$$

where $\phi_{\mathbf{k}}(t) = \phi_{\mathbf{k}}(t + T)$ is periodic and the phase $\epsilon_{\mathbf{k}}$ is the *quasienergy*, which is defined modulo $\Omega = 2\pi/T$. Substituting into the Schrödinger equation gives the eigenvalue problem

$$\mathcal{H}_F \phi_{\mathbf{k}\gamma}(t) \equiv [H(\mathbf{k}, t) - i \partial_t] \phi_{\mathbf{k}\gamma}(t) = \epsilon_{\mathbf{k}\gamma} \phi_{\mathbf{k}\gamma}(t), \quad (\text{A3})$$

where the $\gamma = \{1, 2\}$ distinguishes distinct eigenstates of the *Floquet* Hamiltonian \mathcal{H}_F . Defining $\phi_{\mathbf{k}\gamma}(t) = \sum_n \phi_{\mathbf{k}\gamma}^n e^{in\Omega t}$ and $H(\mathbf{k}, t) = \sum_n H^n(\mathbf{k}) e^{in\Omega t}$ we obtain the frequency representation of Eq. (A3),

$$\sum_{m\beta} \langle \alpha n | \mathcal{H}_F | \beta m \rangle \langle \beta m | \phi_{\gamma}^{\ell} \rangle = \epsilon_{\gamma\ell} \langle \alpha n | \phi_{\gamma}^{\ell} \rangle, \quad (\text{A4})$$

where $\langle \alpha n | \mathcal{H}_F | \beta m \rangle = H_{\alpha\beta}^{n-m} + n\Omega \delta_{\alpha\beta} \delta_{nm}$. We omit the momentum label to simplify expressions when there is no danger of confusion. The quasienergies are $\epsilon_{\alpha n} = \epsilon_{\alpha} + n\Omega$, where n is an integer. For circular polarization, the external driving can be written as $H_{\text{ext}}(t) = iV\sigma^- e^{i\Omega t} - iV\sigma^+ e^{-i\Omega t}$, where $\sigma^{\pm} = (\sigma_x \pm i\sigma_y)/2$. Hence the Floquet matrix corresponding to circular polarization is $[\mathcal{H}_F]_{nm} = \delta_{n,m} H_0 + iV\sigma^- \delta_{n,m-1} - iV\sigma^+ \delta_{n,m+1} - \delta_{nm} n\Omega$ or explicitly,

$$\mathcal{H}_F^{\text{circ}} = \begin{pmatrix} \ddots & & & & & \\ & H_0 + \Omega & iV\sigma^- & 0 & & \\ & -iV\sigma^+ & H_0 & iV\sigma^- & & \\ & 0 & -iV\sigma^+ & H_0 - \Omega & & \\ & & & & \ddots & \end{pmatrix}, \quad (\text{A5})$$

where H_0 is the unperturbed Dirac Hamiltonian. For linear drive $\mathbf{A}(t) = A_0(\cos \Omega t, 0)$ and the external drive is

$H_{\text{ext}}(t) = V\sigma_y \cos \Omega t$ which leads to

$$\mathcal{H}_F^{\text{lin}} = \begin{pmatrix} \ddots & & & & & \\ & H_0 + \Omega & V\sigma_y/2 & 0 & & \\ & V\sigma_y/2 & H_0 & V\sigma_y/2 & & \\ & 0 & V\sigma_y/2 & H_0 - \Omega & & \\ & & & & \ddots & \end{pmatrix}. \quad (\text{A6})$$

In Fig. 1 we have truncated the Floquet matrix to six Fourier modes and obtained the spectrum of the driven system for circular and linear polarization.

APPENDIX B: DYNAMICAL SYMMETRY OF THE SYSTEM

In the basis of the vectors $\{(1 i e^{i\varphi_{\mathbf{k}}})^T / \sqrt{2}, (-1 i e^{i\varphi_{\mathbf{k}}})^T / \sqrt{2}\}$ the unperturbed Hamiltonian is diagonal $\tilde{H}_0 = v|\mathbf{k}| \sigma_z$ and for linear polarization the perturbation takes the form $\tilde{H}_{\text{ext}}(t) = V \cos \varphi_{\mathbf{k}} \cos \Omega t \sigma_z - V \sin \varphi_{\mathbf{k}} \cos \Omega t \sigma_y$, where $\varphi_{\mathbf{k}}$ is the angle of the electron momentum with respect to the polarization which is taken to define the x -axis. For the case of momenta perpendicular to the polarization the Floquet operator is $\tilde{\mathcal{H}}_F^{\text{lin}} = v|k_y| \sigma_z - V \cos \Omega t \sigma_y - i \partial_t$ and its frequency representation is $[\tilde{\mathcal{H}}_F^{\text{lin}}]_{nm} = v|k_y| \delta_{nm} \sigma_z - V(\delta_{n,m-1} + \delta_{n,m+1}) \sigma_y / 2 + n\Omega \delta_{nm}$ or explicitly shown in Eq. (B1). Note that $\tilde{\mathcal{H}}_F^{\text{lin}}$ can be divided into two disconnected blocks (symmetry classes). For example, the states $v|k_y| - \Omega$ and $-v|k_y| + \Omega$ belong to distinct blocks with no matrix element connecting them to any order in perturbation theory and hence they cross. Similarly, the branches $v|k_y|$ and $-v|k_y|$ do not mix to any order in perturbation theory and hence the crossing at $\mathbf{k} = 0$ is also symmetry-protected as concluded in the main text. Finally we note that an electron in the state $\pm v|k_y|$ always changes chirality upon interacting with a linearly polarized photon leaving it in the state $\mp v|k_y|$. This is in contrast to circular polarized photons where there is a finite probability of leaving the electron with the same chirality.

$$\tilde{\mathcal{H}}_F^{\text{lin}} = \begin{pmatrix} \ddots & & & & & & \\ & v|k_y| + \Omega & 0 & 0 & iV/2 & 0 & 0 \\ & 0 & -v|k_y| + \Omega & -iV/2 & 0 & 0 & 0 \\ & 0 & -iV/2 & v|k_y| & 0 & 0 & iV/2 \\ & -iV/2 & 0 & 0 & -v|k_y| & -iV/2 & 0 \\ & 0 & 0 & 0 & iV/2 & v|k_y| - \Omega & 0 \\ & 0 & 0 & -iV/2 & 0 & 0 & -v|k_y| - \Omega \\ & & & & & & \ddots \end{pmatrix}. \quad (\text{B1})$$

In Fig. 3 we have calculated numerically the lowest branch of quasienergies with a truncated Floquet Hamiltonian to six modes as a function of \mathbf{k} for linear polarization. Note that only one branch is independent due to the constraint $\epsilon_{\mathbf{k}1,0} + \epsilon_{\mathbf{k}2,0} = 0$. We have verified numerically the linearity of the dispersion near the band touchings.

APPENDIX C: GAP AT THE DIRAC POINT FROM PERTURBATION THEORY

In the presence of circularly polarized light a gap at $\mathbf{k} = 0$ will develop. It can be understood intuitively as arising from renormalization effects due to virtual interactions between the branches vk and $vk \pm \Omega$. To see this let us consider the truncated Hamiltonian shown in Eq. (8) which contains three branches with Fourier modes $n = 0, \pm 1$. Direct diagonalization involves solving an equation of sixth degree. To reveal the nature of the gap we proceed in a different way. We are only interested in the renormalization of the $n = 0$ mode corresponding to the bands $\pm v|\mathbf{k}|$ near $\mathbf{k} = 0$. The set of equations to solve is (omitting momentum label)

$$(H_0 + \Omega)\phi_\alpha^1 + iV\sigma^-\phi_\alpha^0 = \epsilon_\alpha\phi_\alpha^1, \quad (\text{C1})$$

$$-iV\sigma^+\phi_\alpha^1 + H_0\phi_\alpha^0 + iV\sigma^-\phi_\alpha^{-1} = \epsilon_\alpha\phi_\alpha^0, \quad (\text{C2})$$

$$-iV\sigma^+\phi_\alpha^0 + (H_0 - \Omega)\phi_\alpha^{-1} = \epsilon_\alpha\phi_\alpha^{-1}. \quad (\text{C3})$$

If we assume that $\Omega \gg \epsilon_\alpha$ then from the first and third equations we solve for $\phi_\alpha^{\pm 1}$ as $\phi_\alpha^{\pm 1} = -i(V/\Omega)\sigma^\mp\phi_\alpha^0$. Substituting back into Eq. (C2) we obtain an effective equation for the $n = 0$ state, $(H_0 - V^2\sigma_z/\Omega)\phi_\alpha^0 = \epsilon_\alpha\phi_\alpha^0$. The eigenvalues of the renormalized Hamiltonian are $\pm\sqrt{v^2k^2 + (V^2/\Omega)^2}$ with a gap at $\mathbf{k} = 0$ of magnitude $\Delta_{k=0}^{\text{circ}}/\Omega \approx 2(V/\Omega)^2$, which is $O(V^2)$ as expected.

APPENDIX D: RETARDED GREEN'S FUNCTION IN PERTURBATION THEORY

One can write explicitly the form of the retarded Green's function to first order in perturbation theory. Proceeding in the standard way by first expressing the equation of motion of the evolution operator in the interaction picture and then expanding to first order in V/Ω we obtain $U_{\mathbf{k}}(t, t') \approx e^{-iH_0(\mathbf{k})(t-t')}[1 - i\int_{t'}^t ds H_{\text{ext}}^I(s, t')]$ where H_{ext}^I is the perturbing Hamiltonian in the interaction picture with respect to H_0 . Using the expression $g_{\alpha\beta}^r(\mathbf{k}, t, t') = -i\theta(t-t')U_{\mathbf{k},\alpha\beta}(t, t')$ and expanding the Green's function in Pauli matrices, $g^r = g_0^r + g_i^r\sigma_i$, we obtain for circular polarization

$$g_0^{r,(0)}(k_x, \bar{t}, t_r) = -i\Theta(t_r)\cos(vk_x t_r),$$

$$g_0^{r,(1)}(k_x, \bar{t}, t_r) = -\frac{2iV}{\Omega}\Theta(t_r)\sin(vk_x t_r)\sin\left(\frac{t_r\Omega}{2}\right)\cos(\Omega\bar{t}),$$

where $t_r = t - t'$ and we have retained only the part proportional to the identity as only this part contributes to the spectral function after taking the trace. We have set $k_y = 0$ for simplicity to illustrate our point. After Fourier transforming in t_r we note that to zeroth order, we obtain the usual Dirac-like dispersion $\pm vk_x$ corresponding to the eigenvalues of H_0 and to first order the Green's function is explicitly time periodic in \bar{t} , with sharply defined excitation bands at $\pm vk_x \pm \Omega/2$.

¹D. C. Tsui, H. L. Stormer, and A. C. Gossard, *Phys. Rev. Lett.* **48**, 1559 (1982); G. E. Volovik, *Exotic Properties of Superfluid ³He* (World Scientific, Singapore, 1992); W. P. Su, J. R. Schrieffer, and A. J. Heeger, *Phys. Rev. Lett.* **42**, 1698 (1979).

²M. Z. Hasan and C. L. Kane, *Rev. Mod. Phys.* **82**, 3045 (2010).

³R. Roy, *Phys. Rev. B* **79**, 195322 (2009).

⁴J. E. Moore and L. Balents, *Phys. Rev. B* **75**, 121306 (2007).

⁵L. Fu and C. L. Kane, *Phys. Rev. B* **76**, 045302 (2007).

⁶M. Dzero, K. Sun, V. Galitski, and P. Coleman, *Phys. Rev. Lett.* **104**, 106408 (2010); S. Wolgast, C. Kurdak, K. Sun, J. W. Allen, D.-J. Kim, and Z. Fisk, arXiv:1211.5104; X. Zhang, N. P. Butch, P. Syers, S. Ziemak, R. L. Greene, and J. Paglione, *Phys. Rev. X* **3**, 011011 (2013).

⁷N. H. Lindner, G. Refael, and V. Galitski, *Nat. Phys.* **7**, 490 (2011).

⁸T. Kitagawa, E. Berg, M. Rudner, and E. Demler, *Phys. Rev. B* **82**, 235114 (2010).

⁹M. S. Rudner, N. H. Lindner, E. Berg, and M. Levin, *Phys. Rev. X* **3**, 031005 (2013).

¹⁰M. C. Rechtsman, J. M. Zeuner, Y. Plotnik, Y. Lumer, D. Podolsky, F. Dreisow, S. Nolte, M. Segev, and A. Szameit, *Nature (London)* **496**, 196 (2013).

¹¹T. Kitagawa, T. Oka, A. Brataas, L. Fu, and E. Demler, *Phys. Rev. B* **84**, 235108 (2011).

¹²T. Oka and H. Aoki, *Phys. Rev. B* **79**, 081406 (2009).

¹³Z. Gu, H. A. Fertig, D. P. Arovas, and A. Auerbach, *Phys. Rev. Lett.* **107**, 216601 (2011); B. Dóra, J. Cayssol, F. Simon, and R. Moessner, *ibid.* **108**, 056602 (2012).

¹⁴Y. H. Wang, D. Hsieh, E. J. Sie, H. Steinberg, D. R. Gardner, Y. S. Lee, P. Jarillo-Herrero, and N. Gedik, *Phys. Rev. Lett.* **109**, 127401 (2012).

¹⁵D. Hsieh, D. Qian, L. Wray, Y. Xia, Y. S. Hor, R. J. Cava, and M. Z. Hasan, *Nature (London)* **452**, 970 (2008); Y. Xia, D. Qian, D. Hsieh, L. Wray, A. Pal, H. Lin, A. Bansil, D. Grauer, Y. S. Hor, R. J. Cava *et al.*, *Nat. Phys.* **5**, 398 (2009); H. Zhang, C.-X. Liu, X.-L. Qi, X. Dai, Z. Fang, and S.-C. Zhang, *ibid.* **5**, 438 (2009).

¹⁶S. V. Syzranov, M. V. Fistul, and K. B. Efetov, *Phys. Rev. B* **78**, 045407 (2008).

¹⁷Y. Zhou and M. W. Wu, *Phys. Rev. B* **83**, 245436 (2011).

¹⁸A. Gómez-León and G. Platero, *Phys. Rev. Lett.* **110**, 200403 (2013).

¹⁹Y. H. Wang, H. Steinberg, P. Jarillo-Herrero, and N. Gedik (unpublished).

²⁰L. P. Kadanoff and G. Baym, *Quantum Statistical Mechanics* (Perseus Books, Cambridge, Mass., 1989).

²¹J. H. Shirley, *Phys. Rev. B* **138**, 979 (1965).

²²J. K. Freericks and A. V. Joura, *Electron Transport in Nanosystems* (Springer, Berlin, 2008).

²³T. Dittrich, P. Hänggi, G.-L. Ingold, B. Kramer, G. Shon, and W. Zwerger, *Quantum Transport and Dissipation* (Wiley-VCH, Weinheim, 1998).

²⁴V. Galitski, *Phys. Rev. A* **84**, 012118 (2011); J. H. Wilson, B. M. Fregoso, and V. M. Galitski, *Phys. Rev. B* **85**, 174304 (2012).

²⁵F. Großmann and P. Hänggi, *Europhys. Lett.* **18**, 571 (1992).

²⁶J. K. Freericks, H. R. Krishnamurthy, and T. Pruschke, *Phys. Rev. Lett.* **102**, 136401 (2009).

²⁷P. Delplace, Á. Gómez-León, and G. Platero, arXiv:1304.6272 [cond-mat.mes-hall].